applied sciences

MDPI

Article

Additional Taxi-Out Time Prediction for Flights at Busy Airports by Fusing Flow Control Information

Ligang Yuan [1,2,*], Jing Liu [1,2] and Haiyan Chen [2,3]

[1] College of Civil Aviation, Nanjing University of Aeronautics and Astronautics, Nanjing 211106, China; liujing20010530@163.com
[2] State Key Laboratory of Air Traffic Management System, Nanjing 211106, China; chenhaiyan@nuaa.edu.cn
[3] College of Computer Science and Technology, Nanjing University of Aeronautics and Astronautics, Nanjing 211106, China
* Correspondence: yuanligang@nuaa.edu.cn

Abstract: The taxi-out time of an airport scene can be categorized into the unimpeded taxi-out time and the additional taxi-out time. Usually, additional taxi-out time is used as a key index to monitor taxi-out performance, and its accurate prediction plays an important role in optimizing the allocation of time slots at an airport and improving scene operation efficiency. Taking Shanghai Pudong International Airport as the research object, we first analyze its layout and construct the origin–destination pairs (ODPs) based on the stand groups and runways. Then, we develop a multiple linear regression model based on the arrival and departure flows to calculate the unimpeded taxi-out times for all ODPs. The actual taxi-out time is then subtracted from the unimpeded taxi-out time to obtain the historical additional taxi-out time of each flight. We propose three new flow features related to the structure: the corridor departure flow, the corridor arrival flow, and the departure flow proportion of ODPs, based on which we construct a dataset for training the prediction model. We then propose an additional taxi-out time prediction model based on the nutcracker optimization algorithm (NOA) and XGBoost and run comparison experiments on the operation data of our target airport. The results show that the optimized prediction model we proposed has the best performance compared with the traditional XGBoost model and other commonly used prediction models, and the proposed structure-related features have high correlations with additional taxi-out time.

Keywords: unimpeded taxi-out time; additional taxi-out time; optimization algorithms; corridor; stand group

Citation: Yuan, L.; Liu, J.; Chen, H. Additional Taxi-Out Time Prediction for Flights at Busy Airports by Fusing Flow Control Information. *Appl. Sci.* **2024**, *14*, 9968. https://doi.org/10.3390/app14219968

Academic Editor: Jose Machado

Received: 30 September 2024
Revised: 25 October 2024
Accepted: 28 October 2024
Published: 31 October 2024

1. Introduction

As an important part of airport scene guarantees, the flight taxiing process directly affects a series of work projects such as the construction of the airport collaborative decision-making system (ACDM) and the airport apron handover. The taxi-out time of a flight is the difference between its actual out of block time (AOBT) and its actual take-off time (ATOT). The corresponding taxi-in time is the difference between the actual landing time (ALDT) and the actual in-block time (AIBT) of the flight. Currently, the off-block time for a flight under the domestic ACDM mechanism is obtained by subtracting the estimated taxi-out time from the calculated take-off time (CTOT). However, this estimated taxi-out time is a fixed value that does not take into account factors such as flow of the scene, stands, and runways. This can lead to large deviations between estimated taxi-out times and actual values, affecting the apron rollout sequence as well as the runway queuing sequence. Therefore, accurately predicting flight taxi-out times is beneficial to efficiently scheduling flight departure sequences, shortening waiting time on the ground, reducing flight delays, and increasing passenger satisfaction.

Taxi-out time is divided into unimpeded taxi-out time (UTT) and additional taxi-out time (ATT), as shown in Figure 1. UTT refers to the taxi time of a flight under optimal

operating conditions, e.g., when congestion, convective weather, or other delay causes are not significant [1]. And the ATT is equal to the difference between the total taxi-out time and the UTT, which is an important metric to monitor the taxi performance of an airport. When optimizing taxi times, the goal is to minimize the ATT and fuel consumption, not to reduce it to unimpeded time, which could negatively impact runway throughput. Studying the taxi-out time by dividing it into UTT and ATT not only helps to understand the trend of these two types of time, but also provides a new way of thought for taxi-out time prediction. However, existing studies on taxi time prediction have viewed it as a whole. Moreover, existing research on the factors influencing departure taxi time has only considered macro-level flow and lacks studies on the special structural flow of the airport scene. In terms of prediction methods for departure taxi time, common machine learning algorithms have been utilized without further optimization of their parameters. Additionally, there is a lack of detailed grouping, zonal analysis validation experiments, and ablation experiments in the empirical validation, which limits our understanding of the predictive capabilities for taxi times under different scenarios and conditions. Therefore, it is necessary to conduct more in-depth research to explore the diverse factors affecting departure taxi time, optimize the prediction models, and implement more refined experimental designs to enhance the accuracy and applicability of the predictions.

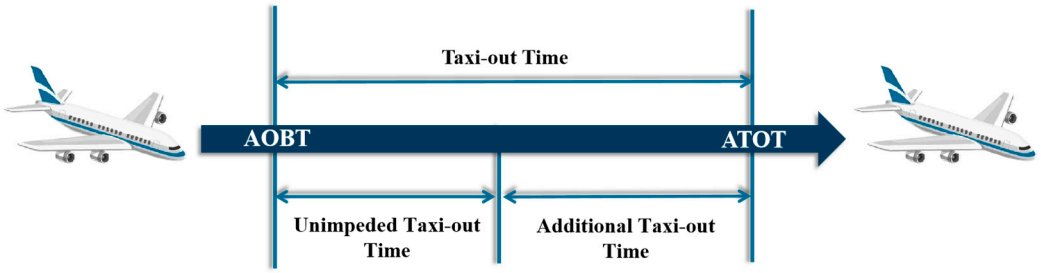

Figure 1. Composition of taxi-out time.

To address the limitations of the existing works, we use a regression model with the highest correlation between departure and arrival flows to calculate the UTT to obtain the ATT, which will be used as the true value in this paper. We then propose three new features related to the structure of the airport for the ATT prediction: corridor departure flow, corridor arrival flow, and departure flow proportion of the ODP, which serve as the basis for constructing the ATT prediction feature set and dataset. Combining the advantages of heuristic algorithms and machine learning algorithms, we propose an ATT prediction model, NOA-XGBoost, in which the NOA algorithm is used to optimize the XGBoost model. Finally, we conduct experiments on the operation data of Shanghai Pudong International Airport to verify the effectiveness of the proposed features and the prediction model.

Through our study, we are able to effectively calculate UTT and ATT for flights and establish a corresponding database, which provides guiding recommendations for taxi time statistics and on-time performance calculation methods in China. Furthermore, the prediction of additional taxi time allows for a more accurate estimation of aircraft pushback times based on CTOT, contributing to the reduction of surface congestion and the improvement of operational efficiency at airports.

The main contributions of this paper can be summarized as follows:

(1) The arrival and departure flows of different ODPs are analyzed, and a multiple linear regression model of taxi-out time is constructed to calculate the UTT.
(2) Three new features are proposed to improve the ATT feature set and dataset: corridor departure flow, corridor arrival flow, and the departure flow proportion of ODP.
(3) An ATT prediction model based on NOA-XGBoost is proposed.
(4) The effectiveness of the proposed features and prediction model is verified through comparative experiments and ablation experiments on the operation data of Shanghai Pudong International Airport.

2. Literature Review

2.1. Related Work

2.1.1. Research on Calculating Unimpeded Taxi-Out Time

The Federal Aviation Administration's (FAA) Aviation Policy and Planning Office (APO) established a linear regression model to calculate UTT [2]. They grouped the flights by airline and season, calculated the number of departure flights and arrival flights in each group, and established a linear regression model for each group. By setting the coefficient of the departure flights queue variable to 1 and the coefficient of the arrival flights queue variable to 0 in the regression model, the UTT can be obtained. EUROCONTROL's European Performance Review Unit (PRU) proposed the concept of a congestion index to calculate UTT [2]. They grouped flights according to certain features, such as aircraft class, entry sector, runway, stand, and so on. Then, they counted the number of all departing and arriving flights during the period from when a flight pushes back to when it takes off, which is defined as the congestion index. Finally, they ranked the taxi times of departing flights in order of magnitude, took the 20th percentile of these times as the UTT, and used it to calculate the congestion threshold. In addition, Lu et al. [3] proposed an improved method for calculating the UTT with the handover point time. There are two phases in the process of an aircraft taxiing, from the ramp to its final arrival at the runway end, separated by the handover point. The first phase is the ramp tower control phase, and the second phase is the ATC tower control phase. To determine the UTT, they performed linear regressions on the departure and arrival flows for these two phases, respectively. They set the departure flow coefficient to 1 and the arrival flow coefficient to 0, and then summed the resulting times for each phase to obtain the final UTT.

The domestic method for calculating the unimpeded taxiing time is the 20th percentile method, in which flights grouped according to certain features are sorted in order from smallest to largest taxiing time, and the value at the 20th percentile is taken as the unimpeded taxiing time. For busy airports with complex scenes and a large number of flights, this method is too simple and rough, leading to inaccurate calculations of the UTT.

2.1.2. Research on Taxi Time Prediction

Research on taxi time prediction can be divided into two aspects: features and methods. In the term of features, an increasing number of features are being applied to taxi-out time prediction. Srivastava et al. [4] proposed a flight taxi time prediction model based on a historical traffic flow database generated from ASDE-X data, considering the number of departure and arrival flights as well as the average departure taxi time of the previous quarter. Liu et al. [5] used multiple linear regression equations to establish an explanatory model for flight taxi-out time, and the experimental results showed that the number of arriving and departing flights, the operating time period, and the departure taxi-out time had a significant correlation. Wang et al. [6] investigated the generalizability of the factors affecting the taxi-out time by selecting a total of three typical airports in Europe and Asia, which are Manchester Airport, Zurich Airport, and Hong Kong International Airport. They used the backward feature elimination algorithm to identify important features affecting taxi-out time, and they applied the random forest (RF) algorithm for prediction. The results indicated that using just a subset of features, such as departure/arrival, distance, total turns, average speed, and number of recent flights, can achieve high prediction accuracy. Zhao et al. [7] proposed three new features for the scene operation environment of Guangzhou Baiyun Airport, which are the number of passing hot spots (HSs), whether they are cross taxiing, and whether they are crossing the runway. Song et al. [8] analyzed the factors affecting taxi-out time prediction at Beijing Capital International Airport by using methods such as feature importance ranking, univariate analysis, and recursive feature elimination. They found that the number of concurrent flights and runway operation modes had a significant impact on the prediction results, while basic features of the flight had a smaller effect. Park et al. [9] studied in detail the effect of weather conditions (wind direction, wind speed, visibility, barometric pressure, and precipitation) on taxi times. The results of the

study showed that wind speed, barometric pressure, and precipitation have a significant effect on the taxi-out and taxi-in times of flights.

In terms of methods, machine learning techniques are widely used for taxi time prediction, including simple linear regression, neural networks, and decision trees. Balakrishna et al. [10] proposed a nonparametric reinforcement learning method to predict and analyze taxi time at Tampa International Airport and the results show that the method achieves 81% prediction accuracy for individual flights within a margin of ±2. Ravizza et al. [11] proposed a taxi time prediction method based on the fuzzy rule system, which was verified to have better performance than multiple linear regression, least median squared linear regression, support vector regression, and M5 model trees on the data of Stockholm Arlanda Airport and Zurich Airport. Lordan et al. [12] used log-linear regression analysis to predict flight taxi-out times and obtained better results. Diana et al. [13] explored linear regression (RL), ridge regression (RR), lasso regression (LR), elasticNet regression (ER), support vector regression (SVR), random forest (RF), adaboost regression (AR), bagging regression (BR), extra trees regression (ETR), and gradient boosting regression tree (GBRT) models for predicting taxi-out time under different datasets. The results show that the ordinary least-squares and ridge models predict relatively well, but no algorithm is suitable for all types of data. Li et al. [14] proposed a deep learning model including a temporal flow sub-model (airport capacity, number of taxiing flight, different time periods), a spatial sub-model (taxiing distances), and an environmental sub-model (weather, air traffic control, runway configurations, aircraft categories) to incorporate the influence of spatiotemporal factors, external environmental conditions, and spatial characteristics by three sub-models. Zhi et al. [15] proposed a taxi-out time prediction model for departure flights based on local weighted support vector regression, and the prediction results show that the accuracy within ±3 min can reach 83.3%, which is better than the traditional support vector regression model. Pham et al. [16] performed the prediction in two stages, first predicting the taxi path of the flight and then predicting the taxi time according to the taxi path and taxi distance. The prediction results show that the accuracy within ±5 min can reach 95%. Xia et al. [17] used a BP neural network model to predict the taxi-out time, and the prediction results of the taxi-out time of departure flight fitted well with the true values. Du et al. [18] innovatively proposed a deep metric learning model to predict taxi time by finding the most similar scenes in the history. They filter out the most similar scenarios, and then calculate the average taxi time as the prediction of the taxi time for the current scenario. Zbakh et al. [19] used a neural network (NN), support vector machines (SVMs), and a regression tree (RT) to predict the taxi-out time at Mohammed V Casablanca Airport and the experimental results show that the prediction performance of the NN is better. This study also found that machine learning models with lower training performance can still show better prediction performance.

From the above research, we can see that the existing works studied the taxi-out time as a whole without considering its components and lacked the optimization of the prediction algorithms in terms of methodology. Based on the above works, in this paper, we propose an ATT prediction model based on the nutcracker optimization algorithm (NOA) and XGBoost. We first calculate the UTT, and then propose three features: the corridor departure flow, the corridor arrival flow, and the departure flow proportion of ODP, and use the NOA algorithm to improve the XGBoost algorithm for ATT prediction.

2.2. Research Gap

We summarize the existing studies in terms of features, research airports, and prediction methods, as shown in Table 1. From Table 1, we can obtain the following conclusions:

(1) The existing studies consider taxi time as a whole [4–19], while not analyzing UTT and ATT separately.
(2) The existing studies consider the flow of the scene as a whole [4–19], without focusing on the flow associated with the microstructure of the scene, such as the flow of the corridor.

(3) Most of the existing prediction methods focus on the comparison of multiple machine learning methods [6,7,11,13,16,19] without optimizing the methods.

Table 1. Summary of research on taxi time prediction.

Reference	Features	Airport	Prediction Method
Balakrishna et al. [10] (2010)	Scene traffic flow	Tampa International Airport	Reinforcement learning
Srivastava et al. [4] (2011)	Taxi distance, number of flights, average taxi time of the previous quarter and weather	John F Kennedy Airport	Linear regression model
Ravizza et al. [11] (2014)	Taxi distance, taxi turning angle, departure or arrival and number of flights	Arlanda Airport and Zurich Airport	Multiple linear regression, least median squared linear regression, support vector regression, M5 model trees, and fuzzy rule-base systems
Lordan et al. [12] (2016)	Gate, runway, departure or arrival, and number of flights	Barcelona-El Prat Airport	Log-linear regression
Diana et al. [13] (2018)	Scene traffic flow, runway configuration, weather, and delay	Seattle-Tacoma International Airport	RL, RR, LR, ER, SVR, RF, AR, BR, ETR, GBRT
Li et al. [14] (2020)	Weather, air traffic flow control, runway configuration, and aircraft category	Hong Kong Airport	Spatiotemporal–environment deep learning model
Xing et al. [15] (2020)	Scene traffic flow, taxi routes, departure waiting queues, and airlines	Unknown	Locally weighted support vector regression
Pham et al. [16] (2019)	Gate, runway, day-of-week, hour, aircraft type, weather, and number of flights	Singapore Changi Airport	RF, LR
Wang et al. [6] (2021)	Airport operational information, congestion, average speed, and weather	Manchester Airport, Zurich Airport and Hong Kong International Airport	Random forest, gradient boosting regression trees, polynomial regression, linear regression, multilayer perceptron
Zhao et al. [7] (2021)	Airline, aircraft type, runway, parking period, number of flight taxiing at the same time on the field, severe weather, length of takeoff queue, cross-taxiing or not, and number of passes through HS	Guangzhou Baiyun International Airport	XGBoost, SVR, RF
Xia et al. [17] (2022)	Scene traffic, taxiing distance, number of turns, delays, and time of day at takeoff time	Unknown	BP
Song et al. [8] (2022)	Surface traffic flow, departure runway, operating load, taxi distance, air route control, and flight properties	Beijing Capital International Airport	GBRT
Du et al. [18] (2022)	Flight properties, surface traffic, and meteorological conditions	Shanghai Pudong International Airport	Deep metric learning approach
Zbakh et al. [19] (2024)	Congestion level, unimpeded taxi-out time, saturation level, and aircraft type	Mohammed V Casablanca Airport	NN, SVM, and RT

In order to fix these problems, we study the UTT and ATT separately and apply NOA to optimize the XGBoost model for taxi time prediction. The gaps between our study and existing works are as follows:

(1) Unlike existing studies that examine taxi-out time as a whole, we separate taxi-out time into UTT and ATT, which allows us to provide detailed analyses and give more accurate predictions.

(2) Compared with existing studies, we focus on the flow of special structural corridors, in addition to the overall flow of the scene, such as the number of departure flights on the scene and the number of arrival flights on the scene. Combining the micro-flow with the macro-flow enables us to capture the impact of the scene flow factors in a more comprehensive way.

(3) We combine the NOA algorithm with the XGBoost algorithm and apply the new intelligent NOA optimization algorithm to optimize multiple parameters of the XGBoost algorithm so as to improve the prediction accuracy.

3. Prediction of Additional Taxi-Out Time

3.1. Layout of Shanghai Pudong Airport

Shanghai Pudong International Airport is one of the three major hub airports in China, with a large number of flights and a complex scene structure, which belongs to typical busy airports, so we take it as the research object. The layout of this airport is shown in Figure 2. The airport has a total of four parallel runways, with the two departure runways, numbered 16R/34L and 17L/35R, highlighted by the red box. The other two unmarked runways are the arrival runways, numbered 16L/34R and 17R/35L. The blue box in the figure outlines 22 different stand groups, where SG is the abbreviation for the stand group. Flights within the same stand group have similar departure and arrival taxiing routes. The two straight lines with red arrows in the figure represent taxiway 3 and taxiway 4, which connect the east and west control zones of the airport. The arrows indicate the direction of the two corridors, and TW stands for the abbreviation of taxiway.

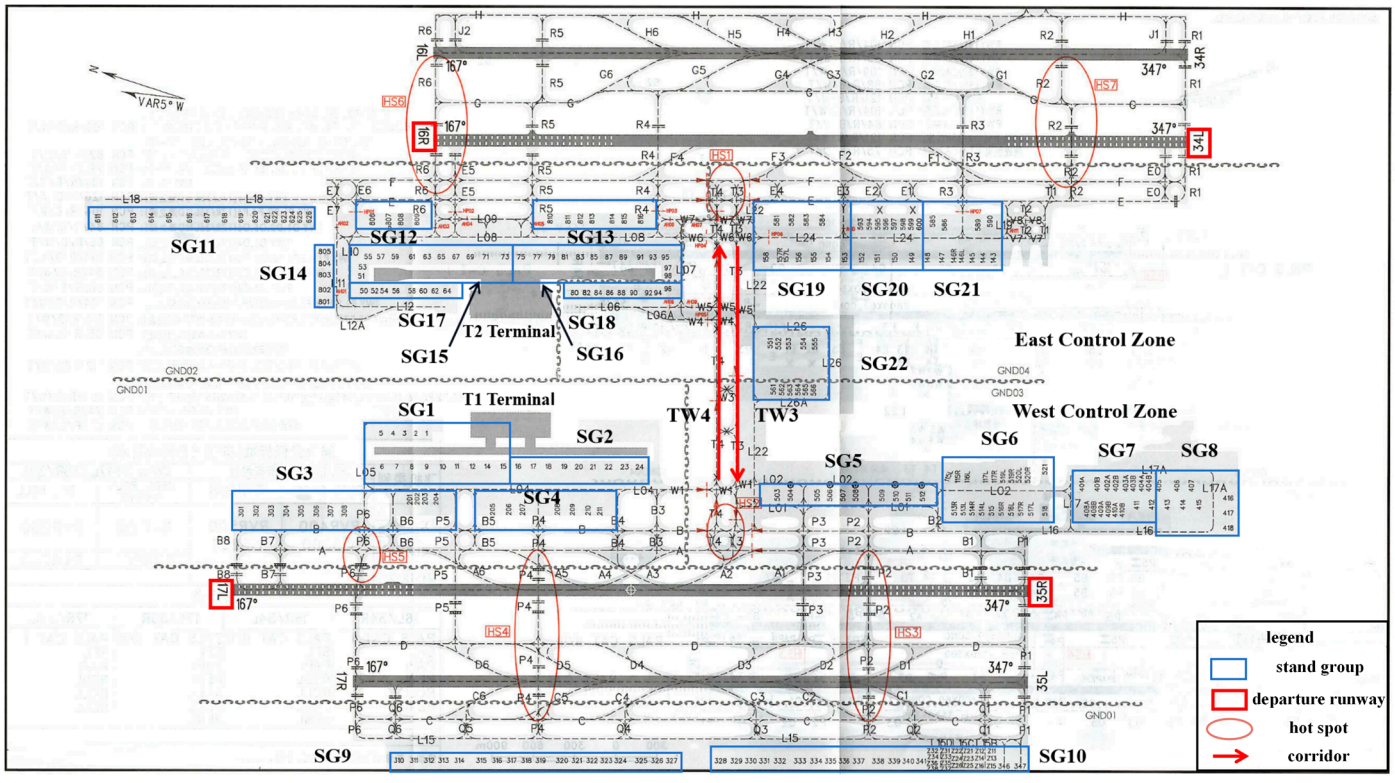

Figure 2. Layout of Pudong International Airport.

3.2. Calculation of UTT

To predict the ATT, first we need to obtain the actual value of the ATT. Since relevant data are not available directly, they can only be calculated by subtracting the UTT from the departure taxi-out time. To calculate the UTT, we use the linear regression-based method developed by the Aviation Policy and Planning Office (APO) of the United States, in which airlines are grouped by using only those that participate in the Airline Service Quality Performance (ASQP) system, while assigning an average value to the other airlines at the airport. This analysis is more applicable to the operational performance of airlines rather than airports. Additionally, for busy multi-runway airports where the distribution of airline parking spots is not significant, this method may lead to an inaccurate calculation of the ATT. Based on this, we propose a method for obtaining the UTT that considers gate groups and runways, as shown in Figure 3. We first pair the twenty-two stand groups with the four departure runways to create eighty-eight origin–destination pairs (ODPs) and calculate the UTT for each ODP. Then, we analyze the arrival and departure flows and select the flow values most strongly correlated with the taxi-out time as explanatory variables. Finally, we establish a regression model to obtain the UTT for each stand group and runway pairing pattern when there are no other departure or arrival flights.

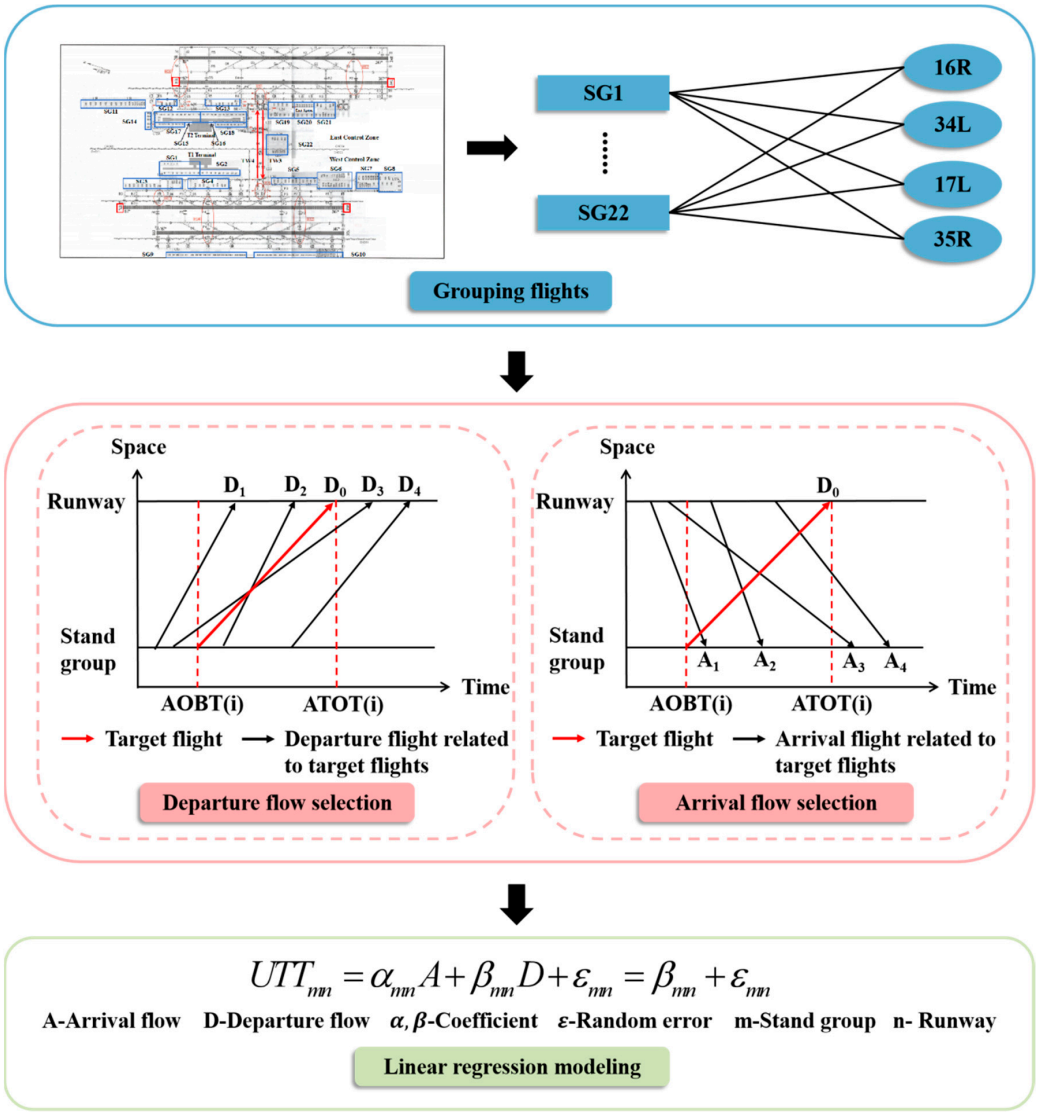

Figure 3. Calculation process of UTT.

3.2.1. Selection of Arrival and Departure Flow Indicators

Pudong International Airport is a busy airport with complex aircraft movements during peak times. It is necessary to select appropriate arrival and departure indicators for fitting the taxi time. For a departing flight i, the other arriving and departing flights that have a temporal interaction with it can be classified into eight types. This forms a set of eight candidate arrival and departure indicators, as shown in Figure 3, for departure flow selection and arrival flow selection, as detailed in Table 2.

Table 2. Candidate set of arrival and departure flow indicators.

Indicator Type	Indicator	Definition
Departure	D1	For a departing flight i, the number of other departure flights j that satisfy $AOBT(j) < AOBT(i)$ & $AOBT(i) < ATOT(j) < ATOT(i)$
	D2	For a departing flight i, the number of other departure flights j that satisfy $AOBT(j) > AOBT(i)$ & $AOBT(i) < ATOT(j) < ATOT(i)$
	D3	For a departing flight i, the number of other departure flights j that satisfy $AOBT(j) < AOBT(i)$ & $ATOT(j) > ATOT(i)$
	D4	For a departing flight i, the number of other departure flights j that satisfy $ATOT(j) > ATOT(i)$ & $AOBT(i) < AOBT(j) < ATOT(i)$
Arrival	A1	For a departing flight i, the number of other arrival flights j that satisfy $ALDT(j) < AOBT(i)$ & $AOBT(i) < AIBT(j) < ATOT(i)$
	A2	For a departing flight i, the number of other arrival flights j that satisfy $ALDT(j) > AOBT(i)$ & $AOBT(i) < AIBT(j) < ATOT(i)$
	A3	For a departing flight i, the number of other arrival flights j that satisfy $ALDT(j) < AOBT(i)$ & $AIBT(j) > ATOT(i)$
	A4	For a departing flight i, the number of other arrival flights j that satisfy $AIBT(j) > ATOT(i)$ & $AOBT(i) < ALDT(j) < ATOT(i)$

Taking ODP SG15-35R as an example, we can apply the Pearson correlation coefficient method to create a correlation heatmap between different arrival and departure flow indicators and taxi-out time, as shown in Figures 4 and 5. The redder the color, the higher the correlation between the indicators and taxi time.

From Figures 4 and 5, it can be seen that D2 has the highest correlation of 0.81 with departure taxi-out time and A2 has the highest correlation of 0.74 with arrival taxi-out time. In contrast, D3 and A3 have the weakest correlation with the departure and arrival taxi-out time. The figures also show the correlations between different indicators. As the number of indicators increase, the correlations with other indicators are also strengthened. For example, the indicator group D1+D2+D3+D4 has a correlation of over 0.6 with 13 other indicators. In the FAA method, departure flow and arrival flow are defined as D1+D3 and A1+A3, respectively. Figures 4 and 5 reveal that both D1+D3 and A1+A3 show low correlations with taxi-out time, at 0.17 and 0.05, respectively. Therefore, we select the indicators D2 and A2 with the highest correlations as the departure flow and arrival flow indicators for linear regression.

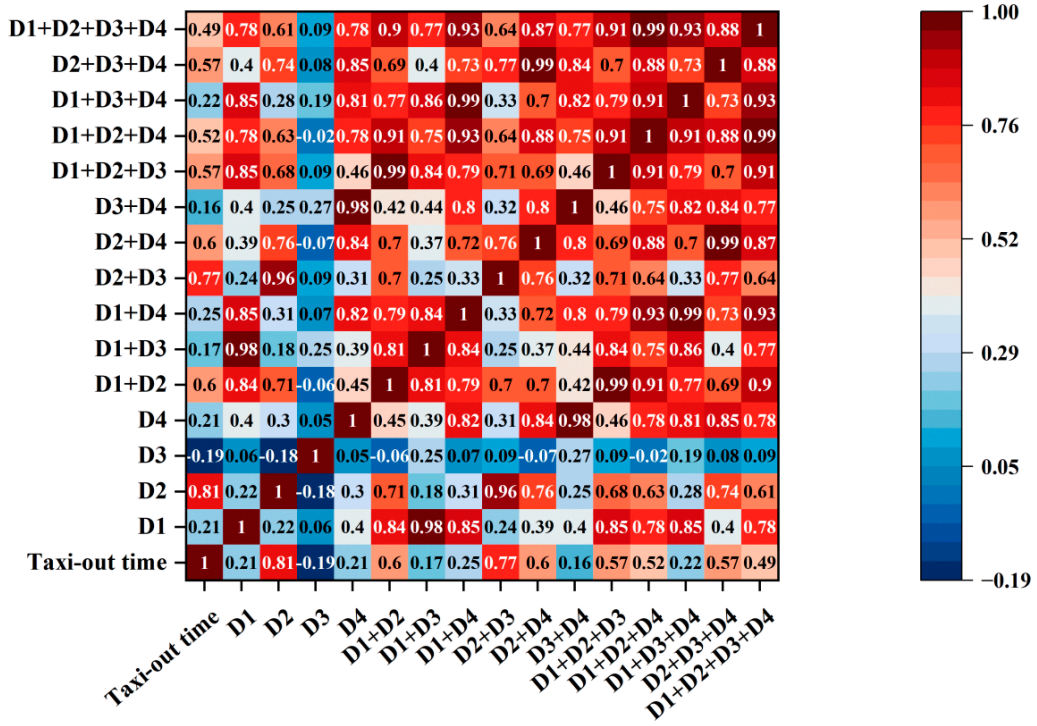

Figure 4. Analysis of departure indicator correlation.

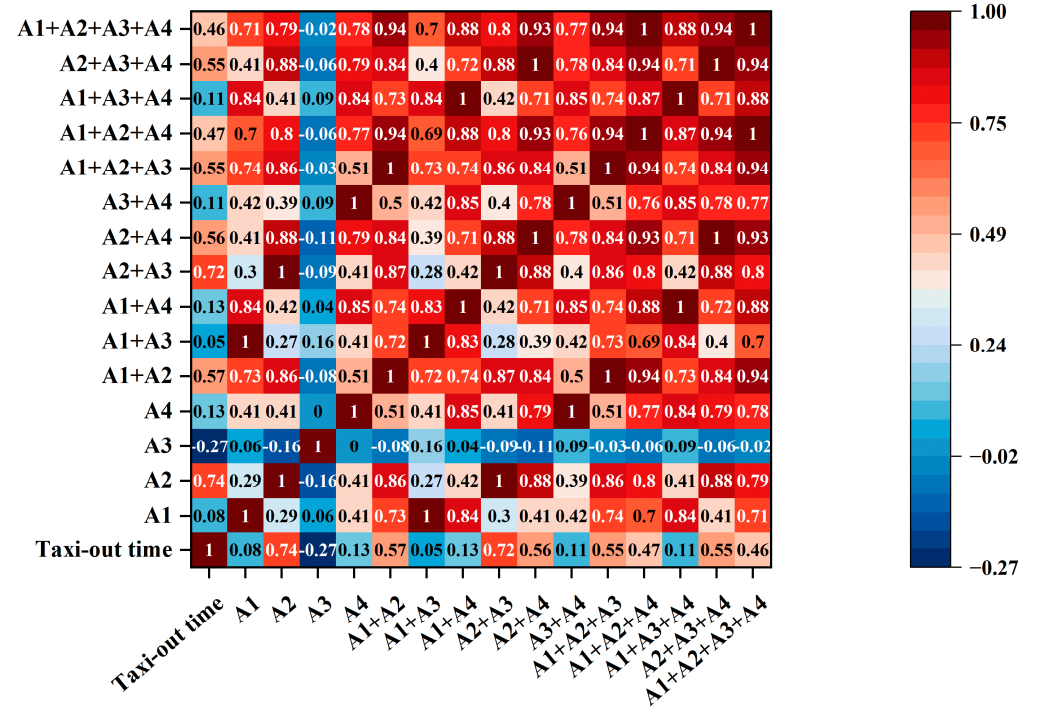

Figure 5. Analysis of arrival indicator correlation.

3.2.2. Calculation Model

We select the departure flow D2 and arrival flow A2, which have the strongest correlation with taxi-out time, as explanatory variables for linear regression, as shown in Equation (1). By setting the coefficient of the departure flow variable to 1 and the coefficient of the arrival flow variable to 0 in the regression model, we obtain the UTT.

$$UTT_{mn} = \alpha_{mn}A + \beta_{mn}D + \varepsilon_{mn} \quad (1)$$

Here, A and D represent arrival flow and departure flow, respectively. α_{mn} and β_{mn} denote the coefficients for arrival flow and departure flow under the pairing of stand group m and departure runway n. ε_{mn} is the random error.

The UTT obtained above is taken as the true value. Subtracting it from the total taxi-out time yields the ATT, which may be used for the subsequent prediction of ATT.

3.3. Prediction of ATT

3.3.1. Construction of Feature Set

For the better prediction of the ATT, we propose three new features related to the structure of the airport: corridor departure flow, corridor arrival flow, and departure flow proportion of ODP.

(1) Corridor flow

As shown in Figure 2, Shanghai Pudong Airport features a unique structure known as the corridor, which is prone to traffic congestion and contributes to an increased ATT. We analyze the trend of the ATT with changes in corridor departure flow and corridor arrival flow, as shown in Figure 6. Corridor departure flow refers to the number of departing flights that taxi from the stand groups in the east (west) control zone through corridor TW3 (TW4) to the departure runways in the west (east) control zone during the taxiing period of the target flight. In contrast, corridor arrival flow refers to the number of arriving flights that land on the arrival runways in the east (west) control zone and then taxi through corridor TW3 (TW4) to the stand groups in the west (east) control zone during the taxiing period of the target flight.

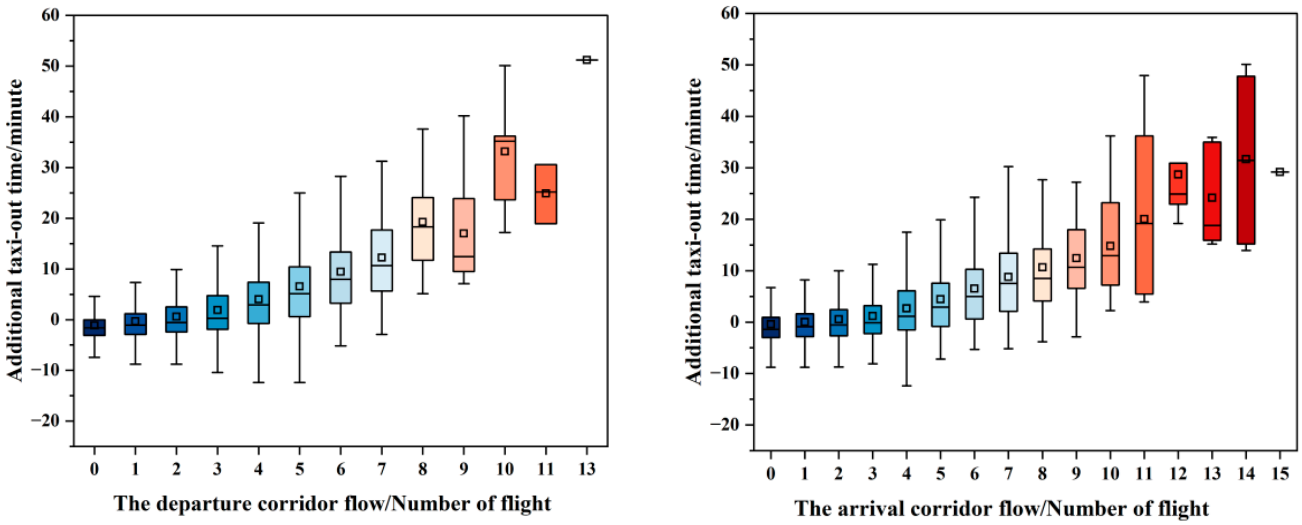

(**a**) (**b**)

Figure 6. Effect of corridor flow on taxi-out time. (**a**) Effect of corridor departure flow; (**b**) effect of corridor arrival flow.

As shown in Figure 6, with the increase in corridor departure flow and corridor arrival flow, the average ATT also rises. When the corridor departure flow and corridor arrival flow values are high, there is some fluctuation in the ATT, but the overall trend remains positively correlated. The main reason is that the number of flights that can pass through the corridor is limited, which means that during peak periods, the flight flow can easily exceed the corridor's capacity. When the corridor flow increases, congestion may occur during the taxiing process, resulting in an increase in the additional taxi-out time for flights.

When the corridor flow values are too high and the scene is in a busy state with complex and intersecting traffic flow information, the ATT becomes more variable, increasing the difficulty of prediction.

(2) Departure Flow Proportion of ODP

This feature indicates the proportion of the departure flow to the total of both departure and arrival flow, as discussed in Section 4. We analyze the trend of the ATT with the proportion of departure flow, as shown in Figure 7, with a Pearson correlation coefficient of 0.49. From the figure, it can be seen that the majority of flights have a low additional taxi-out time, while only a few flights have a higher additional taxi-out time, with their departure flow proportion concentrated between 0.4 and 0.6. This is because when the departure flow proportion is between 0.4 and 0.6, the number of departing flights is close to that of arriving flights, creating a higher mixed state that easily leads to conflicts between flights. Consequently, the taxiing speed is reduced, and the additional taxi-out time increases. In other scenarios, when the departure flow proportion is above 0.6 or below 0.4, the imbalance in the number of departing or arriving flights leads to fewer conflicts, resulting in a relatively faster taxiing speed and, thus, a lower additional taxi-out time.

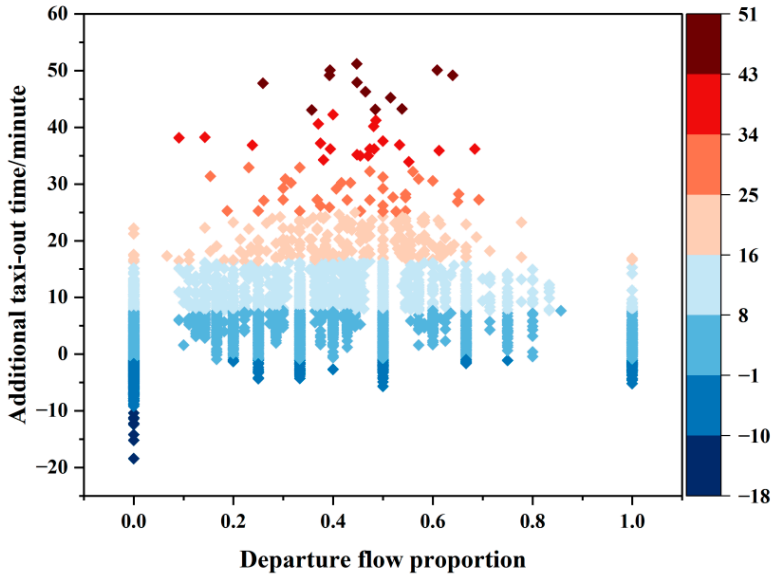

Figure 7. The relationship between departure flow proportion and ATT.

In addition to the three new features mentioned above, we also use 11 additional features, which are shown in Table 3. In Table 3, aircrafts are classified into four categories: C, D, E, and F, primarily based on the standards set forth in the International Civil Aviation Organization (ICAO) Annex to the Convention on International Civil Aviation. Restricted status refers to whether a flight is subject to route traffic restrictions or control area traffic restrictions. Airline, aircraft, and restricted status are encoded using one-hot encoding, where valid feature values are set to 1 and the rest are set to 0.

Table 3. ATT feature set.

Feature Categories		Feature Name
Scene traffic flow	Airline	Domestic airline, foreign airline
	Aircraft	Type C aircraft, type D aircraft, type E aircraft, and type F aircraft
	Restricted status	Restricted flight, unrestricted flight
	Time	Hour
	Normal	Departure flow, arrival flow
	Structure-related	Corridor departure flow, corridor arrival flow, and departure flow proportion of ODP

3.3.2. Construction of Dataset

Based on the feature set constructed in Section 3.3.1, the raw data are preprocessed to construct the ATT dataset. The construction process is shown in Figure 8.

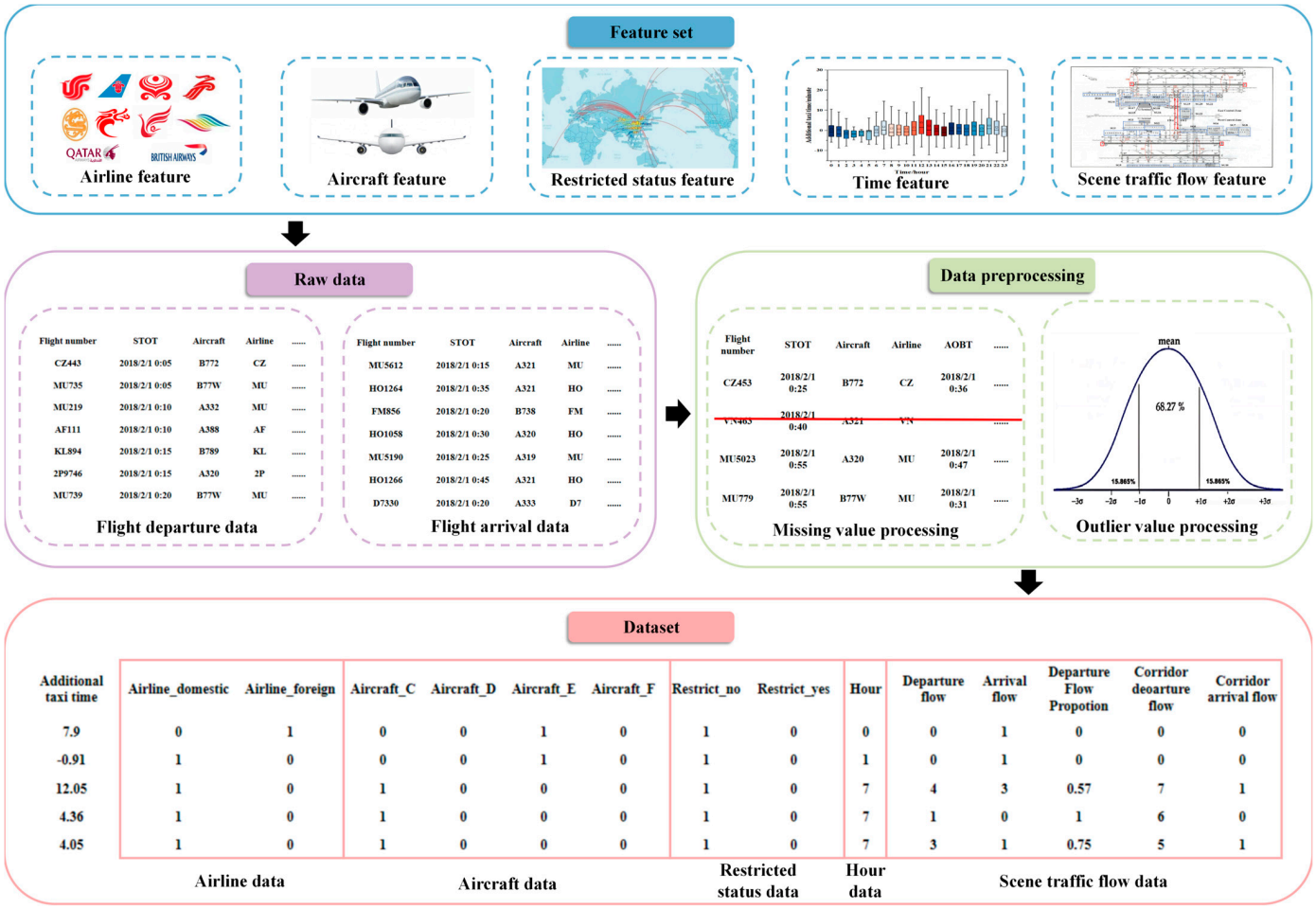

Figure 8. Construction process of the ATT dataset.

First, we select data from the original arrival and departure data according to the feature set, and then we preprocess the raw data. For missing values, since their proportion is small, we directly delete the corresponding data rows. For outliers, we use the standard deviation method to delete data where the taxi-out time exceeds the mean by more than three standard deviations. Finally, we use the preprocessed data to perform calculations based on the meanings of the feature set to obtain the ATT dataset.

3.3.3. Model Construction

Based on the dataset obtained in Section 3.3.2, we propose the NOA-XGBoost model for ATT prediction. First, we split the input dataset into training and testing sets with the ratio 4:1. Then, we initialize the parameters of XGBoost and NOA on the training set, using the RMSE as the fitness function. We apply the NOA algorithm to iteratively update the foraging and storage strategies, as well as the cache-search and recovery strategies, in order to find the optimal XGBoost hyper parameters. Then, we calculate the fitness value and check if the maximum number of iterations has been reached. If so, we proceed to train the NOA-XGBoost model and use it on the testing set to predict the ATT. Otherwise, we continue with the iterative updates. The process of the ATT prediction model based on NOA-XGBoost is as follows. The NOA algorithm consists of two phases: foraging and storage strategies, and cache-search and recovery strategies, with each phase including

global exploration and local exploitation. In the global exploration phase of the foraging and storage strategies, the position update formula is given by Equation (2).

$$\overrightarrow{X}_i^{t+1} = \begin{cases} X_{i,j}^t, & if\ \tau_1 < \tau_2 \\ \begin{cases} X_{m,j}^t + \gamma \cdot (X_{A,j}^t - X_{B,j}^t) + \mu \cdot (r^2 \cdot U_j - L_j), & if\ t \le T_{\max}/2.0 \\ X_{C,j}^t + \mu \cdot (X_{A,j}^t - X_{B,j}^t) + \mu \cdot (r_1 < \delta) \cdot (r^2 \cdot U_j - L_j), & otherwise \end{cases}, & otherwise \end{cases} \tag{2}$$

Here, X_i^{t+1} represents the new position of the i-th nutcracker in the current generation t; $X_{i,j}^t$ represents the j-th position of the i-th nutcracker in the current generation; U_j and L_j are vectors that include the upper and lower bound of the j-th dimension in the optimization problem; γ is a random number generated based on the levy flight; $X_{best,j}^t$ is the currently obtained optimal solution in the j-th dimension; A, B, and C are three different indicators randomly selected from the population to facilitate the exploration of high-quality food sources; $\tau_1, \tau_2,\ r$ and r_1 are random real numbers in the range of [0, 1]; $X_{m,j}^t$ is the mean of all solutions in the j-th dimension in the current population at the t iteration; and μ is generated based on the normal distribution (τ_4), levy flight (τ_5), and randomly between zero and one (τ_3), as shown in Equation (3), where r_2 and r_3 are random real numbers in the range of [0, 1].

$$\mu = \begin{cases} \tau_3, if\ r_1 < r_2 \\ \tau_4, if\ r_2 < r_3 \\ \tau_5, if\ r_1 < r_3 \end{cases} \tag{3}$$

In the local exploitation phase of the foraging and storage strategies, the position update formula is given by Equation (4).

$$\overrightarrow{X}_i^{t+1(new)} = \begin{cases} \overrightarrow{X}_i^t + \mu \cdot (\overrightarrow{X}_{best}^t - \overrightarrow{X}_i^t) \cdot |\lambda| + r_1 \cdot (\overrightarrow{X}_A^t - \overrightarrow{X}_B^t), & if\ \tau_1 < \tau_2 \\ \overrightarrow{X}_{best}^t + \mu \cdot (\overrightarrow{X}_A^t - \overrightarrow{X}_B^t), & if\ \tau_1 < \tau_3 \\ \overrightarrow{X}_{best}^t \cdot l, & otherwise \end{cases} \tag{4}$$

Here, λ is a number generated based on levy flight, τ_3 is a random number between 0 and 1, and l is a factor that linearly decreases from 1 to 0 in NOA exploitation behavior.

In the global exploration phase of the cache-search and recovery strategies, the position update formulas are given by Equations (5)–(7).

$$X_{i,j}^{t+1} = \begin{cases} X_{i,j}^t, & if\ \tau_3 < \tau_4 \\ X_{i,j}^t + r_1 \cdot (X_{best,j}^t - X_{i,j}^t) + r_2 \cdot (\overrightarrow{RP}_{i,1}^t - X_{C,j}^t), & otherwise \end{cases} \tag{5}$$

$$X_i^{t+1} = \begin{cases} X_{i,j}^t, & if\ \tau_5 < \tau_6 \\ X_{i,j}^t + r_1 \cdot (X_{best,j}^t - X_{i,j}^t) + r_2 \cdot (\overrightarrow{RP}_{i,2}^t - X_{C,j}^t), & otherwise \end{cases} \tag{6}$$

$$\overrightarrow{X}_i^{t+1} = \begin{cases} \text{Equation (5)}, & if\ \tau_7 < \tau_8 \\ \text{Equation (6)}, & otherwise \end{cases} \tag{7}$$

Here, $\overrightarrow{RP}_{i+1}^t$ is the first Reference Point (RP) of the current position of the i-th nutcracker in the current t iteration, r_1, r_2, τ_3, τ_4, τ_5 and τ_6 are random numbers between 0 and 1, and C is the index of a solution randomly selected from the population.

In the local exploitation phase of the cache-search and recovery strategies, the position update formulas are given by Equations (8)–(10).

$$\overrightarrow{X}_i^{t+1} = \begin{cases} \overrightarrow{X}_i^t, & if\ f(\overrightarrow{X}_i^t) < f(\overrightarrow{RP}_{i,1}^t) \\ \overrightarrow{RP}_{i,1}^t, & otherwise \end{cases} \tag{8}$$

$$\vec{X}_i^{t+1} = \begin{cases} \vec{X}_i^t, & if\ f(\vec{X}_i^t) < f(\vec{RP}_{i,2}^t) \\ \vec{RP}_{i,2}^t, & otherwise \end{cases} \quad (9)$$

$$\vec{X}_i^{t+1} = \begin{cases} \text{Equation (8)}, & if\ f(\text{Equation (8)} < \text{Equation (9)}) \\ \text{Equation (9)}, & otherwise \end{cases} \quad (10)$$

Here, $\vec{RP}_{i,1}^t$ is the first RP (Reference Point) of the current cache for the i-th nutcracker in the current t iteration, and $\vec{RP}_{i,2}^t$ is the second RP of the current cache for the i-th nutcracker in the current t iteration. All the updates mentioned above must be adjusted according to Equation (11).

$$\vec{X}_i^{t+1} = \begin{cases} \vec{X}_i^{t+1}, & if\ f(\vec{X}_i^{t+1}) < f(\vec{X}_i^t) \\ \vec{X}_i^t, & otherwise \end{cases} \quad (11)$$

After obtaining the optimal XGBoost parameters by reaching the maximum number of iterations, we proceed to train the XGBoost model. First, we initialize the base learners, then calculate the current residuals, train the t-th tree to fit the residuals, and finally update the base learners to complete the training. Subsequently, we use the trained model to make predictions and obtain the predicted values for the ATT. The pseudocode of the NOA-XGBoost algorithm is shown as Algorithm 1.

Algorithm 1. Pseudo-code of NOA-XGBoost

Input: Population size N, upper and lower limits on the value of the XGBOOST hyper parameters L, the current number of iteration t = 0, and the maximum number of iterations $T_{\max}$, training set X_{train}, Y_{train}, test set X_{test}, Y_{test}

Output: Best hyper parameters for the XGBoost model $Best_{hp}$: n_estimators, max_depth, learning_rate, gamma, subsample, colsample_bytree, reg_alpha and reg_lambda, predicted values Y_{pred}

Define the fitness function as the RMSE value
Initialize N nutcracker/solution
Evaluate each solution and find the one with the best fitness in the population
$T = 1$//the current function evaluation//
while $(t < T_{\max})$
  if $\sigma < \sigma_1$//Foraging and storage strategy//
    Updating individual positions using Equations (2), (4) and (11)
  else//Cache-search and recovery strategy//
    Updating individual positions using Equations (7), (10) and (11)
  end if
  Update the current iteration t by $t = t + 1$
end while
Obtain the $Best_{hp}$ for the XGBoost model
Initialize the base learner $h_0(x) = 0$
for t = 1: n_estimators
  for i = 1: len(X_{train}):
  Calculate the residuals $residuals(i) = y_{train}(i) - h_{t-1}(x_i)$
  Train the t-th tree to fit the residuals by using $Best_{hp}$
  Update the base learner $h_t(x_i) = h_{t-1}(x_i) + learning\_rate * h_t(x_i)$
  end for
end for
Use the boosting model to make predictions
for i = 1: len(X_{test}):
  $Y_{pred}(i) = h_t(x_i)$
end for

4. Experiment and Results

4.1. Experimental Setup

To validate the effectiveness and superiority of the proposed NOA-XGBoost-based ATT prediction model, we compare its prediction accuracy with that of XGBoost, RF, and SVR. To study the impact of different types of features on the prediction of the ATT, we use ablation experiments to observe changes in prediction results after removing a certain type of feature. To validate the generalization ability of the proposed prediction model, we predict and analyze the ATT results for different partition pairing methods. To investigate the impact of different traffic indicator calculation nodes on prediction results, we use the calculation nodes in ACDM to compute traffic indicators and make predictions.

We collected flight arrival and departure data from Pudong International Airport from 1 February 2018 to 28 February 2018. After preprocessing, the necessary dataset for the experiment was obtained and then split into a training set and a test set in a 4:1 ratio.

We use five metrics to evaluate the performance of the prediction model: Mean Absolute Error (MAE), Root Mean Square Error (RMSE), Coefficient of Determination (R^2), ± 3 min accuracy, ± 5 min accuracy, and (+5, −10) min accuracy. The expressions for the latter three metrics are shown in Equations (12)–(14). Here, y_i represents the actual value, and $\hat{y}_i$ represents the predicted value. The (+5, −10) min accuracy is a metric established according to domestic airport standards, meaning that the predicted value can be slightly larger than the actual value under the premise of ensuring the flight taxiing.

$$(\pm 3 \text{ min accuracy}) = \frac{\sum_{i=1}^{n} L(\hat{y}_i, y_i)}{n}, L(\hat{y}_i, y_i) = \begin{cases} 0, |y_i - \hat{y}_i| > 3 \\ 1, |y_i - \hat{y}_i| \leq 3 \end{cases} \tag{12}$$

$$(\pm 5 \text{ min accuracy}) = \frac{\sum_{i=1}^{n} L(\hat{y}_i, y_i)}{n}, L(\hat{y}_i, y_i) = \begin{cases} 0, |y_i - \hat{y}_i| > 5 \\ 1, |y_i - \hat{y}_i| \leq 5 \end{cases} \tag{13}$$

$$(+5, \ -10 \text{ min accuracy}) = \frac{\sum_{i=1}^{n} L(\hat{y}_i, y_i)}{n}, L(\hat{y}_i, y_i) = \begin{cases} 0, -10 \leq y_i - \hat{y}_i \leq 5 \\ 1, \quad otherwise \end{cases} \tag{14}$$

The initial parameters for the NOA and XGBOOST algorithms are shown in Table 4.

Table 4. Algorithm parameter settings.

Model	Parameter	Value
NOA	Population size	50
	Maximum iterations	100
XGBOOST	N estimators	100
	Max depth	6
	Learning rate	0.3
	Gamma	0
	Subsample	1
	Colsample bytree	1
	Reg alpha	0
	Reg lambda	1

4.2. Results and Discussion

4.2.1. Performance Comparison of Different Prediction Models

To validate the effectiveness of the proposed NOA-XGBoost model, we compare it with commonly used taxi-out time prediction methods RF, SVR, and the traditional XGBoost algorithm. The results are shown in Table 5 and Figure 9.

Table 5. Performance of four prediction models.

Model Based	MAE	RMSE	R^2	±3 min Accuracy	±5 min Accuracy	(+5, −10) min Accuracy
NOA-XGBOOST	2.06	2.73	0.77	0.77	0.94	0.97
XGBOOST	2.15	2.85	0.75	0.76	0.93	0.96
RF	2.25	2.95	0.73	0.73	0.92	0.95
SVR	2.27	3.19	0.69	0.73	0.92	0.95

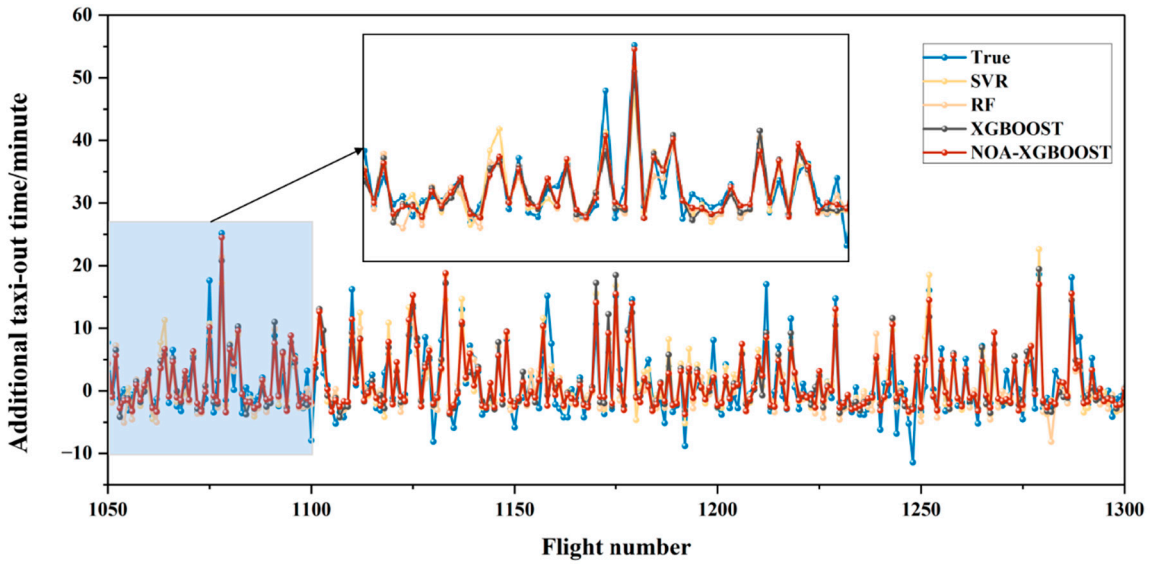

Figure 9. Prediction results of different models.

As seen in Table 5, the NOA-XGBoost algorithm outperforms other algorithms across all six metrics. Compared to the XGBoost model, it improves MAE, RMSE, R^2, ±3 min accuracy, ± 5 min accuracy, and (+5, −10) min accuracy by 4.19%, 4.21%, 2.67%, 1.32%, 1.08%, and 1.04%, respectively. This indicates that optimizing XGBoost parameters using the NOA algorithm can enhance its prediction accuracy and precision. Compared to the RF model, the NOA-XGBoost algorithm improves MAE, RMSE, R^2, ±3 min accuracy, ±5 min accuracy, and (+5, −10) min accuracy by 8.44%, 7.46%, 5.48%, 5.48%, 2.17%, and 2.11%, respectively. Compared to the SVR model, the NOA-XGBoost algorithm shows better performance, with improvements in MAE, RMSE, R^2, ±3 min accuracy, ±5 min accuracy, and (+5, −10) min accuracy of 9.25%, 14.42%, 11.59%, 5.48%, 2.17%, and 2.11%, respectively.

Figure 9 shows the prediction results for flight numbers 1050 to 1300, with an enlargement of the prediction results for 100 flights numbered 1050 to 1100. The enlarged view indicates that the NOA-XGBoost model provides the best fitting results.

4.2.2. Prediction with Different Features

To investigate the impact of different types of features on the experimental results, we conduct feature ablation experiments using the NOA-XGBOOST algorithm. This involved removing one type of feature at a time and observing the changes in results. The outcomes are shown in Table 6 and Figure 10.

As shown in Table 6, removing any one of the features such as airline, aircraft, restriction status, or time results in only a minor decrease in the metrics. This indicates that these features have relatively small impacts on the prediction of the ATT. However, removing the traffic flow features causes a significant drop in performance. When using the traffic flow features, MAE, RMSE, R^2, ±3 min accuracy, ±5 min accuracy, and (+5, −10) min accuracy are improved by 16.3%, 19.47%, 18.46%, 8.45%, 5.62%, and 3.19%, respectively. Similarly, removing the structure-related features proposed in this study also results in a noticeable drop in performance. MAE, RMSE, R^2, ±3 min accuracy, ±5 min accuracy, and

(+5, −10) min accuracy can be improved by 7.62%, 6.51%, 10%, 4.05%, 3.30%, and 3.19%, respectively, by applying the newly proposed features.

Table 6. Prediction performance under different features.

Features Removed	MAE	RMSE	R^2	±3 min Accuracy	±5 min Accuracy	(+5, −10) min Accuracy
None	2.06	2.73	0.77	0.77	0.94	0.97
Airline category	2.07	2.74	0.76	0.76	0.94	0.97
Aircraft category	2.09	2.75	0.76	0.75	0.93	0.96
Restricted status category	2.07	2.75	0.75	0.75	0.93	0.95
Time category	2.07	2.74	0.77	0.75	0.93	0.96
Normal features of scene traffic flow	2.46	3.39	0.65	0.71	0.89	0.94
Structure-related features	2.23	2.92	0.70	0.74	0.91	0.94

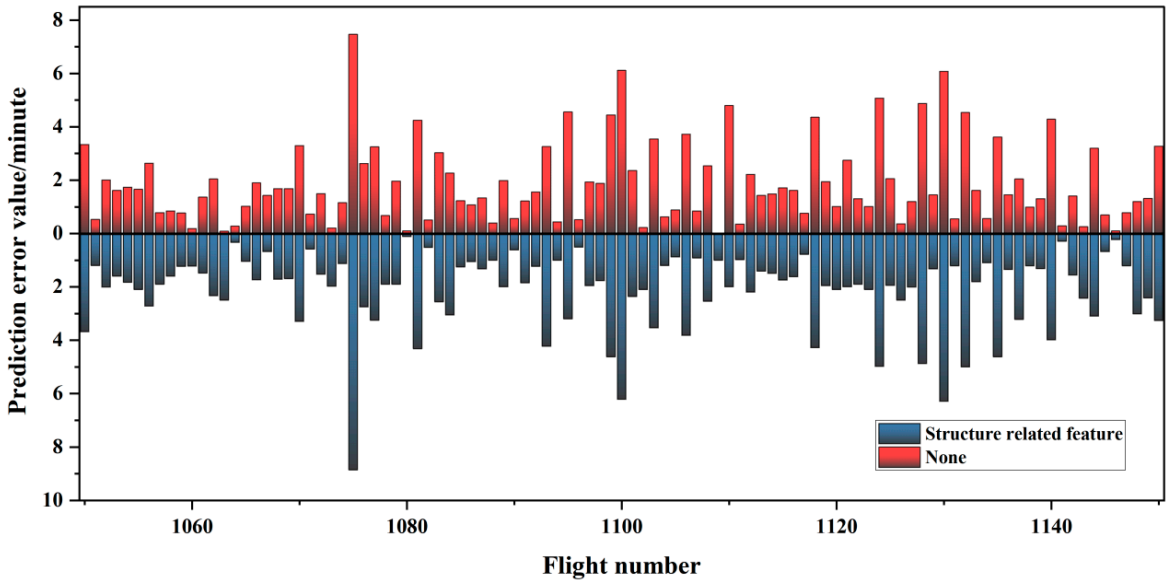

Figure 10. Prediction error comparison.

Figure 10 shows the comparison of the absolute prediction errors for flights numbered 1050 to 1150, with and without the structure-related features. The blue area represents the errors without the new features, while the red area represents the errors with all features. It is obvious that the blue area is larger than the red area, which indicates that the proposed features are effective in improving the prediction performance.

4.2.3. Prediction for Different Pairing Method

To study the algorithm's adaptability and the ATT for cross-corridor and non-cross-corridor pairing methods, this section focuses on predictions using different region and runway pairing methods. The results are shown in Table 7 and Figure 11.

Table 7. Prediction results of different pairing methods.

Pairing Method	Model Based	MAE	RMSE	R^2	±3 min Accuracy	±5 min Accuracy	(+5, −10) min Accuracy
East Control Zone-16R34L	XGBOOST	2.35	3.31	0.80	0.74	0.89	0.94
	NOA-XGBOOST	2.23	3.14	0.82	0.76	0.91	0.94
	RF	2.33	3.31	0.80	0.72	0.90	0.94
	SVR	2.69	4.22	0.68	0.67	0.87	0.92

Table 7. *Cont.*

Pairing Method	Model Based	MAE	RMSE	R^2	±3 min Accuracy	±5 min Accuracy	(+5, −10) min Accuracy
East Control Zone-17L35R	XGBOOST	1.96	2.54	0.51	0.79	0.95	0.97
	NOA-XGBOOST	1.83	2.40	0.56	0.83	0.96	0.98
	RF	2.01	2.59	0.49	0.76	0.94	0.97
	SVR	2.15	2.90	0.37	0.75	0.93	0.96
West Control Zone-16R34L	XGBOOST	2.53	3.49	0.66	0.70	0.90	0.94
	NOA-XGBOOST	2.23	3.19	0.72	0.77	0.91	0.95
	RF	2.47	3.37	0.68	0.72	0.90	0.94
	SVR	2.97	4.11	0.53	0.61	0.84	0.91
West Control Zone-17L35R	XGBOOST	1.98	2.75	0.60	0.77	0.95	0.98
	NOA-XGBOOST	1.95	2.67	0.62	0.80	0.95	0.98
	RF	2.09	2.96	0.54	0.75	0.95	0.97
	SVR	2.25	3.53	0.35	0.75	0.92	0.98

From the Table 7, it can be seen that among the four methods, the NOA-XGBoost model performs the best. The ±3 min accuracy for the NOA-XGBoost method is around 80%, ±5 min accuracy is around 90%, and (+5, −10) min accuracy can reach 95%.

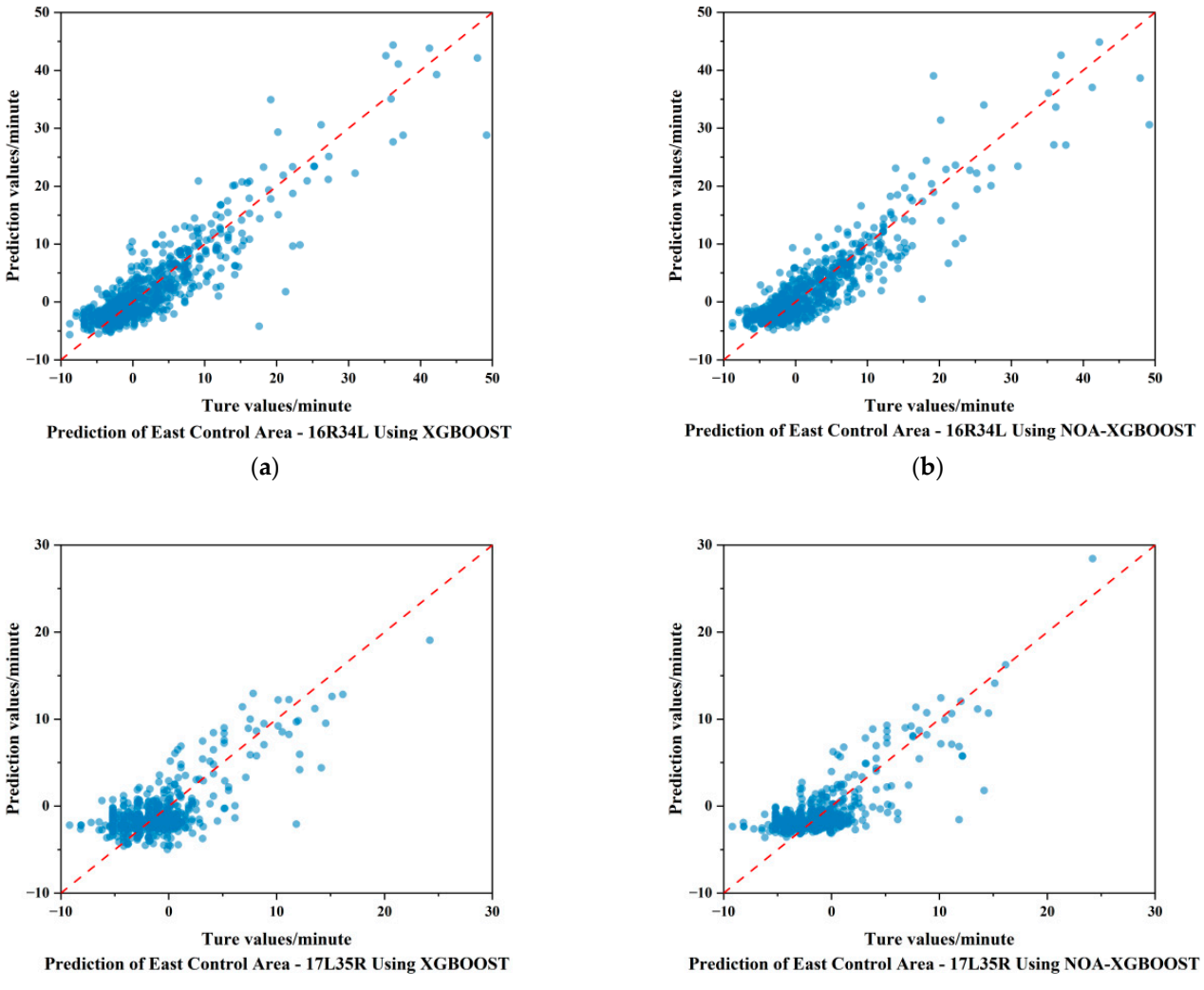

Figure 11. *Cont.*

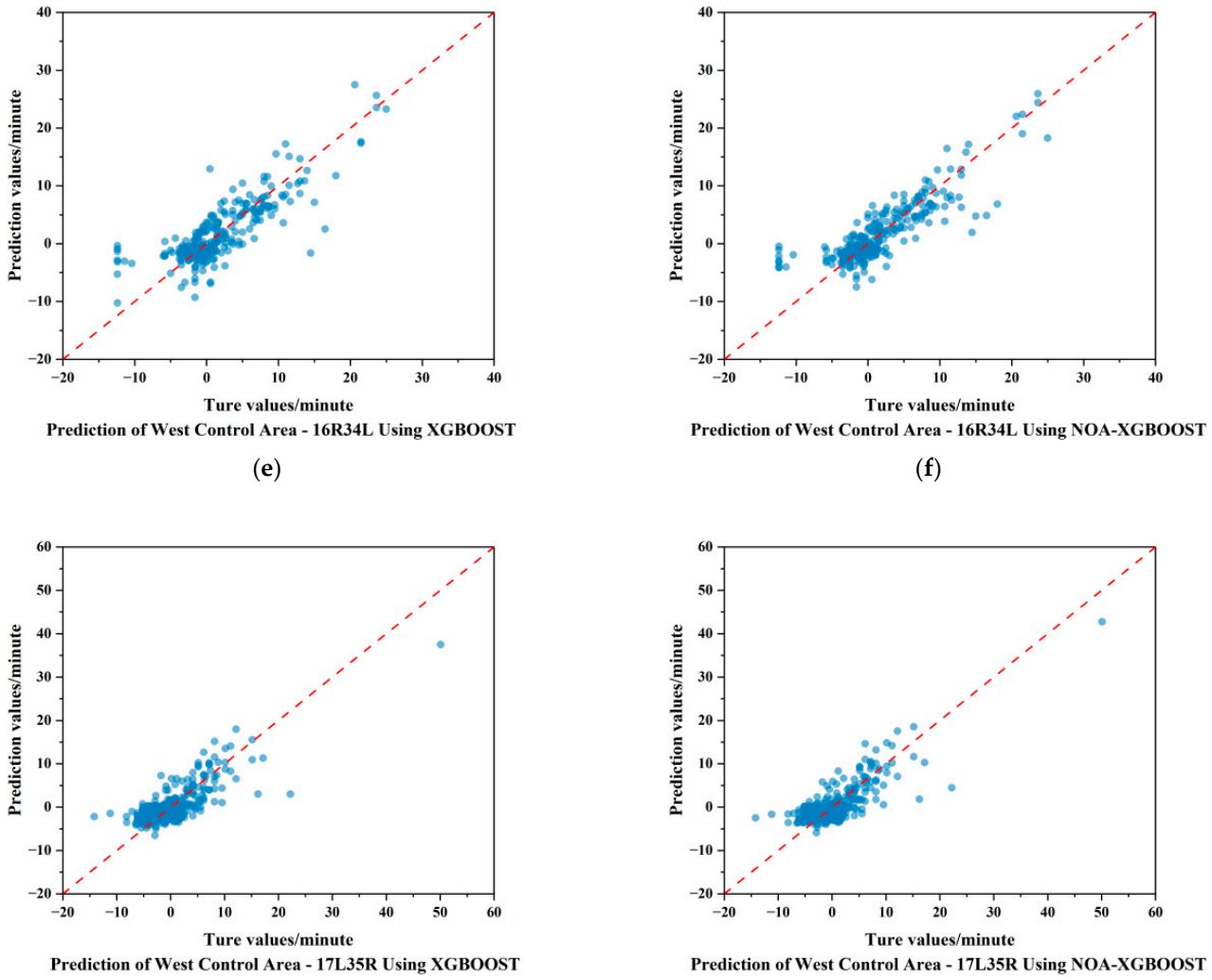

Figure 11. Prediction performance of different pairing methods under different approaches: (**a**) Prediction of East Control Area—16R34L Using XGBOOST; (**b**) Prediction of East Control Area—16R34L Using NOA-XGBOOST; (**c**) Prediction of East Control Area—17L35R Using XGBOOST; (**d**) Prediction of East Control Area—17L35R Using NOA-XGBOOST; (**e**) Prediction of West Control Area—16R34L Using XGBOOST; (**f**) Prediction of West Control Area—16R34L Using NOA-XGBOOST; (**g**) Prediction of West Control Area—17L35R Using XGBOOST; (**h**) Prediction of West Control Area—17L35R Using NOA-XGBOOST.

To investigate the features and prediction effects of the ATT under different pairing methods, we compare the prediction results of the XGBoost algorithm with those of the NOA-XGBoost algorithm, as shown in Figure 11. In the figure, the x-axis represents the actual values, the y-axis represents the predicted values, and the red dashed line represents the function $y = x$. The closer the data points are to this line, the better the prediction performance. Among the four pairing methods, East Control Zone-17L35R and West Control Zone-16R34L are cross-corridor methods, characterized by longer taxiing paths and a higher likelihood of conflicts during taxiing, leading to greater uncertainty and prediction difficulty. As a result, the ATT is longer and the data distribution is more scattered compared to the other two non-cross-corridor pairing methods. Comparing the two algorithms, it can also be observed that for all four pairing methods, the data using the NOA-XGBoost algorithm are closer to the red dashed line than those using the XGBoost algorithm, demonstrating the superiority of the NOA-XGBoost algorithm.

4.2.4. Prediction Based on ACDM Calculation Time

To investigate the impact of different traffic indicator calculation nodes on prediction results, in this section, we use the calculation time points CTOT, COBT, CLDT, and CIBT from the ACDM system as nodes for calculating traffic indicators. These values are typically determined within 30 min to 1 h before flight departure. The results of ATT prediction using these indicators are shown in Table 8.

Table 8. Prediction performance based on ACDM calculation time.

Model Based	MAE	RMSE	±3 min Accuracy	±5 min Accuracy	(+5, −10) min Accuracy
NOA-XGBOOST	3.94	5.62	0.51	0.74	0.85
XGBOOST	4.04	5.82	0.51	0.72	0.84
RF	4.21	6.06	0.49	0.71	0.84
SVR	4.17	6.21	0.53	0.72	0.82

From Table 8, it can be observed that the NOA-XGBoost algorithm proposed in this paper performs the best, with a ±3 min accuracy of 51% and a (+5, −10) min accuracy of 85%. This prediction accuracy is lower compared to the results in Section 4.2.1, with a reduction of 33.77% for ±3 min accuracy and 12.37% for (+5, −10) min accuracy. This discrepancy is due to the deviation between the calculation time nodes in ACDM and the actual time nodes. Although the accuracy has decreased, the (+5, −10) min accuracy still reaches 85%, which is within the acceptable error range for domestic flight operation management.

5. Conclusions

Predicting ATT can reduce taxi wait times and overall delays, while optimizing resource allocation by better managing the use of airport runways, taxiways, and gates, thus improving the overall operational efficiency of the airport. Therefore, we proposed the NOA-XGBoost algorithm to predict the ATT.

First, we established an effective multiple linear regression model by selecting departure and arrival indicators to calculate the UTT. Then, we obtained the true values of ATT through an indirect method. For ATT, we proposed three new features: corridor departure flow, corridor arrival flow, and departure flow proportion of ODP. We then constructed a dataset and proposed the NOA-XGBoost model to predict the ATT. Finally, we conducted an experimental analysis using Shanghai Pudong International Airport as a case study. The comparison of different methods demonstrated the effectiveness of the proposed approach. Ablation experiments on features confirmed the validity of the proposed features. Predictions using different pairing methods provide data features for corridor and non-corridor scenarios, validating the algorithm's adaptability.

By dividing taxi-out time into the UTT and ATT, we can analyze the influencing factors of different times separately, leading to a more comprehensive and in-depth study and optimization of airport ground operations, thereby improving the overall efficiency and safety of the aviation traffic system. Additionally, predicting the ATT rather than the total taxi-out time allows for a more precise reduction of delay times and provides a new perspective for predicting taxi times.

Our research still has certain limitations. For example, the analysis and validation are only conducted for Shanghai Pudong International Airport, and the impact of weather factors on departure taxi time is not considered. Severe weather conditions, such as thunderstorms, snowstorms, and heavy rain, may significantly affect taxi times. In future research, we plan to extend the study to more airports with different surface layouts, such as Guangzhou Baiyun International Airport and Beijing Daxing International Airport, while also introducing additional feature variables to further refine the feature set for predicting departure taxi times.

Author Contributions: Conceptualization, L.Y.; methodology, L.Y. and J.L.; software, J.L.; formal analysis, J.L.; investigation, L.Y. and H.C.; resources, L.Y.; data curation, J.L.; writing—original draft preparation, J.L. and L.Y.; writing—review and editing, L.Y., J.L. and H.C.; supervision, L.Y. and H.C.; project administration, L.Y.; funding acquisition, L.Y. All authors have read and agreed to the published version of the manuscript.

Funding: This paper is supported by the National Key R&D Program of China (No.2021YFB1600500).

Institutional Review Board Statement: Not applicable.

Informed Consent Statement: Not applicable.

Data Availability Statement: The raw data supporting the conclusions of this article will be made available by the authors on request.

Acknowledgments: We would like to thank the State Key Laboratory of Air Traffic Management System for providing the data used in the model tests described in this paper.

Conflicts of Interest: The authors declare no conflicts of interest.

References

1. ASPM Taxi Times: Definitions of Variables. Available online: https://aspm.faa.gov/aspmhelp/index/ASPM_Taxi_Times__Definitions_of_Variables.html (accessed on 10 September 2024).
2. FAA. EUROCONTROL Performance Review Commission and Federal Aviation Administration Air Traffic Organization System Operations Services. U.S./Europe Comparison of 2010 ATM-Related Operational Performance. March 2012. Available online: https://www.faa.gov/air_traffic/publications/media/us_eu_comparison_2010.pdf (accessed on 10 September 2024).
3. Lu, H.; Zhao, Z. Refined evaluation method for aircraft unimpeded taxi-out time. In Proceedings of the 2022 4th International Academic Exchange Conference on Science and Technology Innovation (IAECST), Guangzhou, China, 9–11 December 2022.
4. Srivastava, A. Improving departure taxi time predictions using ASDE-X surveillance data. In Proceedings of the 2011 IEEE/AIAA 30th Digital Avionics Systems Conference, Seattle, WA, USA, 16–20 October 2011.
5. Liu, J.; Yin, M.; Zhu, X. Research on departure influencing factors based on aircraft taxiing out time. *J. Wuhan Univ. Technol. Transp. Sci. Eng.* **2018**, *42*, 195–200.
6. Wang, X.; Brownlee, A.E.I.; Woodward, J.R. Aircraft taxi time prediction: Feature importance and their implications. *Transp. Res. Part C Emerg. Technol.* **2021**, *124*, 102892. [CrossRef]
7. Zhao, Z.; Feng, S.; Song, M. Research on dynamic taxi time prediction method for aircraft based on XGBoost. *Adv. Aeronaut. Sci. Eng.* **2021**, *13*, 76–85.
8. Song, J.; Tang, Y.; He, J. Importance and Prunability Analysis of Basic Features in Machine-Learned Aircraft Taxi-Out Time Prediction. In Proceedings of the International Conference on Green Intelligent Transportation System and Safety, Qinhuangdao, China, 16–18 September 2022.
9. Park, D.K.; Kim, J.K. Influential factors to aircraft taxi time in airport. *J. Air Transp. Manag.* **2023**, *106*, 102321. [CrossRef]
10. Balakrishna, P.; Ganesan, R.; Sherry, L. Accuracy of reinforcement learning algorithms for predicting aircraft taxi-out times: A case-study of Tampa Bay departures. *Transp. Res. Part C Emerg. Technol.* **2010**, *18*, 950–962. [CrossRef]
11. Ravizza, S.; Chen, J.; Atkin, J.A.; Stewart, P.; Burke, E.K. Aircraft taxi time prediction: Comparisons and insights. *Appl. Soft Comput.* **2014**, *14*, 397–406. [CrossRef]
12. Lordan, O.; Sallan, J.M.; Valenzuela-Arroyo, M. Forecasting of taxi times: The case of Barcelona-El Prat airport. *J. Air Transp. Manag.* **2016**, *56*, 118–122. [CrossRef]
13. Diana, T. Can machines learn how to forecast taxi-out time? A comparison of predictive models applied to the case of Seattle/Tacoma International Airport. *Transp. Res. Part E Logist. Transp. Rev.* **2018**, *119*, 149–164. [CrossRef]
14. Li, N.; Jiao, Q.; Zhu, X. Prediction of departure aircraft taxi time based on deep learning. *Trans. Nanjing Univ. Aeronaut. Astronaut.* **2020**, *37*, 232–241.
15. Zhi, W.; Jiang, S.; Qian, L. Prediction of flight taxi-out time in a busy airport based on LWSVR. *J. Syst. Simul.* **2020**, *32*, 927–935.
16. Pham, D.T. A data-driven approach for taxi-time prediction: A case study of Singapore Changi airport. In Proceedings of the 6th ENRI International Workshop on ATM/CNS (EIWAC2019), Nakano, Japan, 29–31 October 2019.
17. Xia, Z.; Jia, X. Taxi-out time prediction of departure aircraft based on BP neural network. *Adv. Aeronaut. Sci. Eng.* **2022**, *13*, 99–106.
18. Du, J.; Hu, M.; Zhang, W. Finding Similar Historical Scenarios for Better Understanding Aircraft Taxi Time: A Deep Metric Learning Approach. *IEEE Intell. Transp. Syst. Mag.* **2022**, *15*, 101–116. [CrossRef]
19. Zbakh, D.; El Gonnouni, A.; Benkacem, A. Taxi-out time prediction at Mohammed V Casablanca Airport. *Int. J. Electr. Comput. Eng.* **2024**, *14*, 2126–2134. [CrossRef]